Environ. Sci. Technol. **2005**, *39,* 4599−4605

Chromium-Removal Processes during Groundwater Remediation by a Zerovalent Iron Permeable Reactive Barrier

RICHARD T. WILKIN,* CHUNMING SU, ROBERT G. FORD, AND CYNTHIA J. PAUL
U.S. Environmental Protection Agency, Office of Research and Development, National Risk Management Research Laboratory, 919 Kerr Research Drive, Ada, Oklahoma 74820

Solid-phase associations of chromium were examined in core materials collected from a full-scale, zerovalent iron permeable reactive barrier (PRB) at the U.S. Coast Guard Support Center located near Elizabeth City, NC. The PRB was installed in 1996 to treat groundwater contaminated with hexavalent chromium. After eight years of operation, the PRB remains effective at reducing concentrations of Cr from average values >1500 μg L^{-1} in groundwater hydraulically upgradient of the PRB to values <1 μg L^{-1} in groundwater within and hydraulically downgradient of the PRB. Chromium removal from groundwater occurs at the leading edge of the PRB and also within the aquifer immediately upgradient of the PRB. These regions also witness the greatest amount of secondary mineral formation due to steep geochemical gradients that result from the corrosion of zerovalent iron. X-ray absorption near-edge structure (XANES) spectroscopy indicated that chromium is predominantly in the trivalent oxidation state, confirming that reductive processes are responsible for Cr sequestration. XANES spectra and microscopy results suggest that Cr is, in part, associated with iron sulfide grains formed as a consequence of microbially mediated sulfate reduction in and around the PRB. Results of this study provide evidence that secondary iron-bearing mineral products may enhance the capacity of zerovalent iron systems to remediate Cr in groundwater, either through redox reactions at the mineral−water interface or by the release of Fe(II) to solution via mineral dissolution and/or metal corrosion.

Introduction

Chromium is a common groundwater contaminant at hazardous waste sites where subsurface contamination stems from industrial processes such as metal plating, leather tanning, and pigment production. Passive, in situ reactive barriers have proven to be viable, cost-effective systems for remediation of Cr-contaminated groundwater at some sites (*1*). Permeable reactive barriers (PRBs) are installed in the flow-path of groundwater, most typically as vertical treatment walls (*2*, *3*). Redox-active solids used in PRBs, such as zerovalent iron (ZVI), promote rapid removal of redox-sensitive contaminants, such as Cr, by various mechanisms including adsorption and reductive precipitation. Further development of PRB technology to improve long-term performance, reduce operation and maintenance costs, and to plan post-remediation activities requires a better understanding of the mechanisms responsible for contaminant removal in and around reactive barriers. ZVI has been used in full-scale PRB systems for the treatment of metal contaminants such as Cr (*4*−*6*) and U (*7*, *8*). In addition, benchtop laboratory studies with ZVI have been carried out to evaluate treatment effectiveness and reaction processes for a selection of metal contaminants including, for example, Cr (*9*−*17*), U (*18*, *19*), As (*20*−*24*), and Zn (*25*−*27*).

In ZVI treatment systems, the removal mechanism for hexavalent Cr, the more soluble and toxic form of Cr, is believed to involve reduction of Cr(VI) to Cr(III), coupled with the oxidation of Fe(0) to Fe(II) and Fe(III) and the subsequent precipitation of sparingly soluble Fe(III)−Cr(III) oxyhydroxides or hydroxides. Laboratory batch and column tests show that reacted iron filings develop coatings of goethite (α-FeOOH) with Cr concentrated at the outermost grain boundaries (*13*). Surface analytical techniques indicate that Cr in the solid phase is present as Cr(III), supporting the reductive precipitation mechanism. Therefore, the working model for Cr removal in ZVI PRBs, based upon laboratory observations, is via the formation of a solid solution or by adsorption of Cr(III) onto the surfaces of iron corrosion products. Investigations in less ideal field systems, however, have revealed considerable complexity with respect to mineralogical endpoints that result from the interactions between groundwater, ZVI granules, and subsurface biota (*28*−*33*). For example, neoformed minerals identified in materials collected from field installations of ZVI include a range of iron carbonate, hydroxy-carbonate, (oxy)hydroxide, oxide, and sulfide minerals, all of which could be involved in Cr removal via adsorption and/or reductive precipitation.

The PRB installed at the U.S. Coast Guard Support Center located near Elizabeth City, NC, is a well documented full-scale ZVI PRB designed and constructed for the removal of Cr(VI) from groundwater (*4*, *5*, *30*, *31*, *34*, *35*). The Elizabeth City PRB was installed in June of 1996 with dimensions 46 m long, 7.3 m deep, and 0.6 m wide. Since installation of the PRB, a detailed monitoring study has been carried out consisting of groundwater analysis, mineralogical and microbiological characterization of core materials, and geochemical modeling (*35*). The objective of this study is to gain a better understanding of the geochemical processes that control the transformation and removal of dissolved Cr(VI) from a groundwater contaminant plume that is being treated by a passive, in situ permeable reactive barrier. Assessment of the long-term performance of the PRB and stability of Cr in the reactive material requires an understanding of the mechanisms responsible for Cr removal.

Materials and Methods

Core Samples. Core samples characterized in this study were collected at the Elizabeth City site in July 2001 and September 2003 by using direct-push coring equipment (Geoprobe; Salina, KS). Angled cores (30° from vertical) were retrieved in regions upgradient, within, and downgradient of the PRB containing ZVI granules (*36*). Precautions were taken to minimize oxidation of saturated aquifer and reaction zone materials. Cores were frozen immediately after collection and shipped in ice chests packed with dry ice. The cores were thawed and processed in a Coy anaerobic chamber containing 2−5% (v/v) H_2 and less than 1 ppmv O_2. Core processing and solid-phase analytical methods are described in the Supporting Information.

* Corresponding author phone: (580) 436-8874; fax: (580) 436-8703; e-mail: wilkin.rick@epa.gov.

10.1021/es050157x CCC: $30.25
Published on Web 04/30/2005

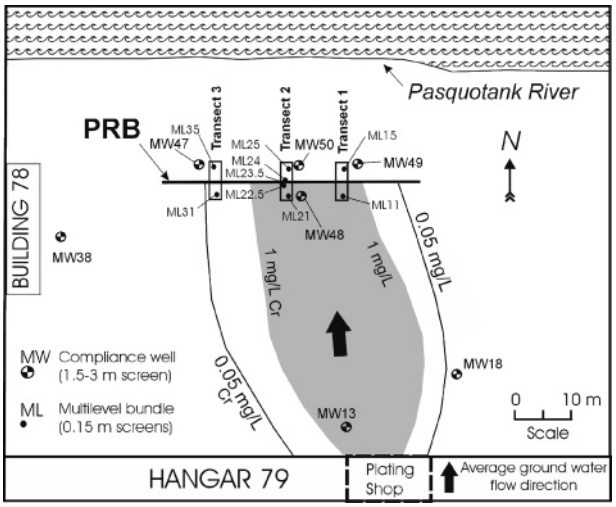

FIGURE 1. Schematic site map showing locations of the groundwater Cr plume, the ZVI PRB, and the network of groundwater monitoring wells discussed in the text. Transect 2 is composed of five multilevel well bundles located upgradient (ML21, ML22.5, ML23.5), within (ML24), and downgradient (ML25) of the PRB.

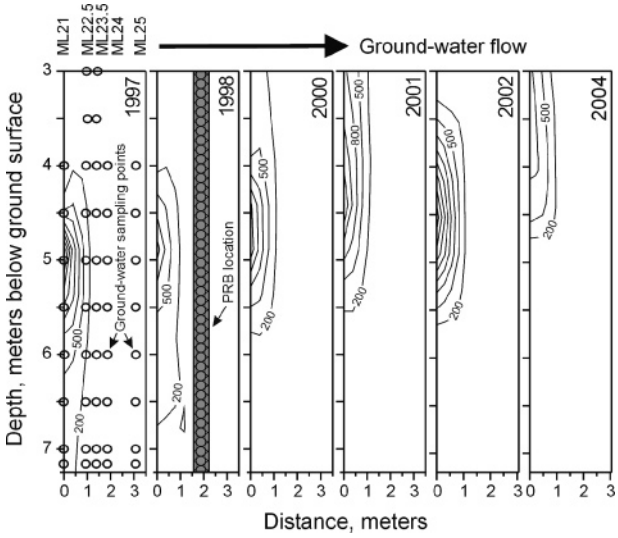

FIGURE 2. Cross-sectional profiles showing the concentration distribution of total Cr in groundwater relative to the position of the PRB. Data collected in 1999 and 2003 are not shown. Contours are based on concentration data from 44 subsurface sampling points in transect 2 (see Figure 1). The contour interval is 300 μg Cr L^{-1}.

Groundwater Collection. Groundwater samples were collected from a network of 159 monitoring wells located upgradient, within, and downgradient of the reactive barrier and at depths from approximately 3−19 m below ground surface (see Figure 1, ref *37*). All groundwater collection and analysis procedures are described elsewhere (*37*). Concentrations of total Cr were determined by inductively coupled plasma optical emission spectroscopy (ICP-OES) at concentrations >10 μg L^{-1} and by ICP mass spectrometry at lower concentrations (ICP-MS; Thermo Elemental PQExcell; minimum detection limit 0.05 μg L^{-1}). These methods have precisions of 10% or better for the groundwater samples analyzed. Concentrations of hexavalent chromium were measured in the field using the 1,5-diphenylcarbazide colorimetric indicator and a spectrophotometer (HACH DR/2010). The minimum detection limit for this method was 20 μg L^{-1}.

Cr K-Edge X-ray Absorption Near-Edge Structure (XANES) Spectroscopy Analysis. The oxidation state and bonding environment of Cr associated with the aquifer materials and fine-grained fraction recovered from ZVI samples was examined using XANES spectroscopy. Cr K-edge spectra were collected at beamline 20-BM (PNC Collaborative Access Team) at the Advanced Photon Source, Argonne National Laboratory (Argonne, IL). Samples were loaded into 1.5-mm-thick plastic sample holders and sealed with strips of Kapton tape. All sample and mineral reference solids were handled in a N_2-filled glovebag to minimize oxidation of Cr and other redox-sensitive elements. Absorption spectra were collected at the Cr edge (5989 eV) in fluorescence mode using a 13-element solid-state Ge detector. Samples were mounted at 45° with respect to the incident beam. The energy of a Si(111) double-crystal monochromator was calibrated using Cr foil inserted between the second and third ionization chambers. A He plus N_2 gas mixture was used in the first ionization chamber, and N_2 gas was used in the second and third chambers. The monochromator step size was 0.25 eV per step in the XANES region (5968−6038 eV). Multiple scans were collected and summed for each sample (3−9). Step counting time was varied between 2 and 10 s to improve the signal-to-noise ratio for samples with variable Cr concentrations. The XANES K-edge inflection point was determined as the energy at the maximum in the first derivative of the normalized spectra.

For comparison purposes, mineral reference compounds were synthesized in the laboratory (e.g., ferrihydrite, lepidocrocite, siderite, carbonate green rust, and mackinawite) in systems containing Cr as $Na_2CrO_4 \cdot 4H_2O$ or $CrCl_3 \cdot 6H_2O$. Synthesis methods and mineralogical characterization results are presented in the Supporting Information (Table S1 and Figure S1).

Scanning Electron Microscopy/Energy Dispersive X-ray Spectrometry (SEM/EDS). Samples were examined with a JEOL JSM-6360 Scanning Electron Microscope at an accelerating voltage of 25 kV and a beam current of about 10 nA. The microscope is equipped with an Oxford Instruments Model 6587 energy dispersive spectrometer with high-resolution lithium-drifted silicon detectors. Samples for SEM and EDX analysis were stored in an anaerobic glovebox and then embedded in an epoxy resin. The sample mounts (1-in. diameter round mounts) were ground and polished using diamond abrasives and coated with a thin layer of gold prior to being placed within the SEM sample chamber.

Results and Discussion

Cr Remediation through Time. Over the eight-year period from 1996 to 2004, there were a total of 23 sampling events in monitoring wells MW47, MW49, and MW50, all located hydraulically downgradient of the PRB (Figure 1). Dissolved Cr concentrations measured in groundwater from these wells never exceeded 5 μg L^{-1}. Similarly, in multilevel well bundles ML15, ML25, and ML35 positioned downgradient of the PRB, Cr concentrations were below 5 μg L^{-1} in 117 of 119 sampling events. The highest concentration of total Cr observed in a well-positioned downgradient of the PRB from 1996 to 2004 was 6 μg L^{-1}, significantly below the maximum concentration limit (MCL) and target treatment level for Cr of 100 μg L^{-1}. Analyses by ICP-MS indicate average Cr concentrations in downgradient wells and wells positioned within the ZVI barrier of 0.88 μg L^{-1} (n = 58) and 0.72 μg L^{-1} (n = 14), respectively. A trend of decreasing remedial performance of the PRB, e.g., evidenced by increasing Cr concentrations within the reaction zone or at downgradient locations, is not evident after eight years of operation.

A more detailed picture of contaminant behavior can be drawn by inspecting 2-dimensional concentration profiles, constructed by contouring monitoring data from the multilevel well bundles. Shown in Figure 2 are cross-sectional

profiles of dissolved Cr from 1997 to 2004 in transect 2 at the Elizabeth City PRB. Note that when concentrations of total Cr are greater than 20 μg L^{-1}, Cr is present in the hexavalent oxidation state. Total Cr is highly correlated with Cr(VI) in regions >1 m upgradient of the PRB ($r = 0.96$, $n = 58$; MW13, MW48, and ML21). Long-term trends indicate that Cr continues to be removed from the groundwater plume after eight years of operation. In general, depth-dependent concentration profiles have remained consistent with time but with subtle variations. Contouring results presented in Figure 2 suggest that the depth of the Cr plume has progressively decreased at a rate of approximately 0.1 m $year^{-1}$, and Cr concentrations entering the PRB appear to be decreasing with time. Cr removal from groundwater occurs at or just upstream of the leading edge of the PRB (*35*). The concentration of dissolved Cr entering the PRB is greatest near the location of ML21 (average concentration 827 μg L^{-1}) and least near ML31 on the west side of the PRB (average concentration 60 μg L^{-1}).

Taking an average Cr concentration of 500 μg L^{-1} over the depth interval from 3 to 6 m below ground surface and an average flow velocity of 0.16 m d^{-1} (*4*), it is estimated that the PRB removes about 4.1 kg Cr per year, or about 33 kg of Cr is estimated to have been removed from the groundwater plume and sequestered into immobile forms in the solid phase after eight years. By assumption that this quantity of Cr is partitioned into a Cr-free, dominantly quartz aquifer over the depth interval from 3 to 6 m below ground surface (porosity $\approx$ 0.3) and within 1 m of the upgradient PRB edge, the total Cr concentration in the solid phase is not expected to exceed about 200 μg g^{-1}. Although a number of simplifications are made in order to reach this value, this calculation illustrates that solid-phase concentrations of Cr are not expected to be large even in areas witnessing the maximum rate of Cr uptake.

Long-term trends in groundwater pH and Eh show minimal changes (Supporting Information, Figure S2). In transect 2, the high pH zone caused by corrosion of the ZVI has remained largely unchanged in space over the initial eight-year period of operation (9.5 $\pm$ 0.6, transect 2). This result indicates that the ZVI at Elizabeth City remains reactive even after eight years of subsurface exposure. Transects 1 and 3 also show fairly consistent patterns in pH. Notable is a relatively narrow zone near the influent side of the PRB where increases of 3−4 pH units are observed; a steep gradient in pH has been observed in each sampling event since 1996. Similarly a gradient in the oxidation−reduction potential coincides with the pH gradient. Overall, reducing to moderately reducing conditions that support sulfate-reduction have been maintained in the PRB, although there possibly exists a trend of increasing oxidation−reduction potential with time (Supporting Information, Figure S2). Continued Cr removal from groundwater is largely a function of favorable and stable geochemical conditions that have been maintained after introduction of ZVI to the subsurface.

Mineral Precipitation. Corrosion of iron metal results in a moderately alkaline and reducing geochemical environment that drives abiotic mineral precipitation reactions and supports a variety of microbial metabolic pathways (*38*, *39*). Mineralogical characterization of core materials indicates the formation of calcite/aragonite, iron carbonate hydroxide, magnetite, lepidocrocite, ferrihydrite, mackinawite, and carbonate green rust in the PRB at Elizabeth City (*30*, *31*, *35*). Figure 3 shows solid-phase concentrations of inorganic carbon and total sulfur within the PRB in the direction of groundwater flow as a function of time. Mineral precipitation mainly occurs near the upgradient edge of the PRB, although there is an indication that a precipitation front is progressively moving through the PRB. After eight years of operation, less than 15% of the available pore space has been lost due to

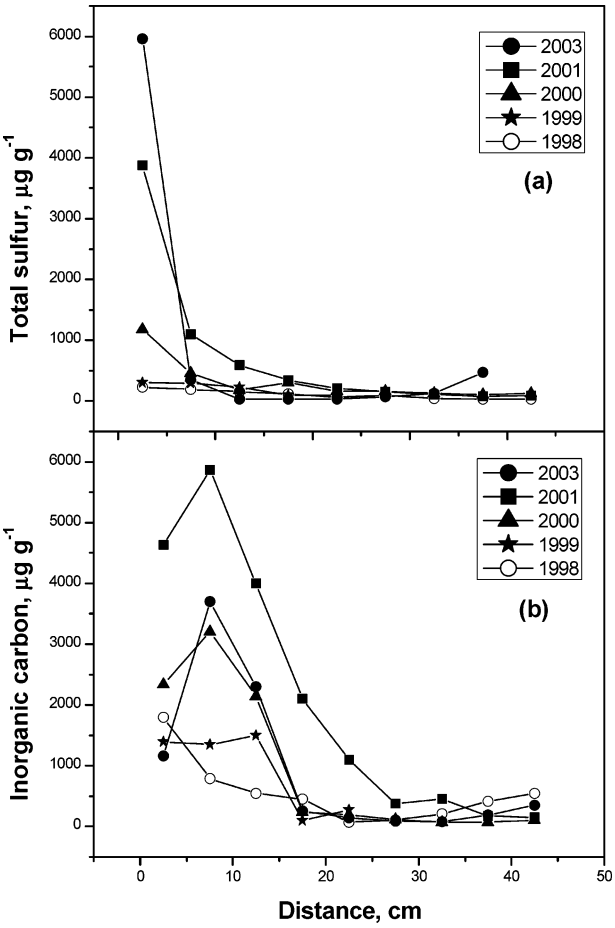

FIGURE 3. Concentrations of (a) total sulfur and (b) inorganic carbon in core materials collected from the Elizabeth City PRB. The origin approximates the contact between the upgradient aquifer and the PRB. Measured concentration profiles are adjusted to reflect horizontal penetration along an axis parallel to groundwater flow (*31*). All cores were collected from approximately the same location and handled using identical preservation and characterization methods.

mineralization near the upgradient edge. Iron core collected near the downgradient edge of the PRB contains very little if any mineral precipitate mass. Near the downgradient edge, <1% of the available pore space has been lost after eight years (*35*). Loss of pore space in ZVI barriers is primarily due to infilling by carbonate precipitates, sulfide precipitates, and the products of iron-metal oxidation (*35*). Overall there appears to be a regular increase with time in the amount of inorganic carbon and sulfide precipitates. The continued buildup of mineral precipitates is believed to negatively impact the hydraulic performance of PRBs (*40*). On the other hand, as discussed below, precipitation of redox-active minerals plays a role in providing additional system capacity for removing Cr(VI) from groundwater.

XANES Analysis. XANES spectroscopy is used here to probe possible solid-phase associations of Cr by comparing spectra of known Cr-bearing reference materials with spectra of unknown samples collected from the Elizabeth City site. Cr K-edge XANES spectra for reference materials are shown in Figure 4. The individual reference materials are arranged to show an increasing energy shift of the Cr absorption edge position from 5989 eV for Cr(0) to 6003.2−6004.3 eV for Cr-(III) associated with iron-bearing minerals and finally to 6007.5 eV for Cr(VI) which additionally shows a characteristic pre-edge feature and adsorption maximum at approximately 5993 eV (Figure 4). The K-edge data exhibit an absorption edge shift of about 3.2 eV per unit oxidation state change for

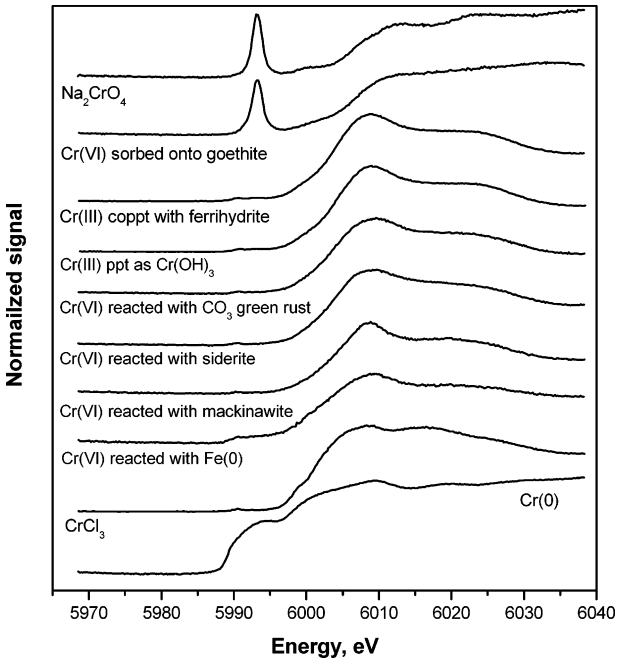

FIGURE 4. Chromium K-edge XANES spectra of model compounds.

Cr. Note that Cr-bearing ZVI, mackinawite, siderite, and carbonate green rust were all prepared in the laboratory using sodium chromate as the Cr source (see Supporting Information, Table SI1). These Fe(II)- and/or mixed Fe(II)−Fe(III)-bearing phases were highly effective in reducing Cr(VI) to Cr(III). This behavior contrasts, for example, with goethite (α-FeOOH) that was exposed to sodium chromate. Only Cr(VI) on goethite is indicated by Cr K-edge XANES analysis, thus highlighting the important role that reduced, solid-phase iron plays in transforming the Cr oxidation state from the hexavalent form to the trivalent form (*12*−*15*, *41*−*43*).

Cr K-edge XANES spectra are shown for four samples in Figure 5a. In these samples, collected from within the reactive medium and from aquifer environments upgradient of the PRB, the absorption edge energy varies from 6004 to 6005 eV (Table 1). Total Cr concentrations in the samples shown in Figure 5a range from about 100 to 815 $\mu g\ g^{-1}$ and are in broad agreement with the predicted concentration range in the solid-phase based on observed decreases in groundwater chromium concentrations. The observed edge positions and the lack of any significant pre-edge feature in the spectra indicate that Cr is present dominantly as Cr(III), confirming the expectation that reductive processes are responsible for Cr removal in and around the PRB. Noticeable differences are apparent in the first derivative data for the reference solids and field samples (Figure 5b). The first derivative data suggest a close similarity in the electronic and structural environment of Cr between the field samples and Cr associated with mackinawite, especially for sample EC01-7-1. In this sample, the total sulfur concentration was 0.16 wt %, of which >90% is present as acid-volatile sulfide consistent with the presence of mackinawite. This is significant because several studies have demonstrated that Cr(VI) is rapidly transformed to insoluble Cr(III) as a result of reactions with iron sulfide surfaces (*44*−*46*).

Microscopy. Microscopic characterization of core materials indicates that mineral accumulation within the PRB occurs mainly on the surfaces of iron granules but also as free mineral precipitates not directly attached to iron grains. After eight years, mineral coverage on iron granules near the upgradient edge of the PRB is regular and approximately 30−150 μm thick. Near the downgradient edge, coverage of the iron grains is less continuous, and where present mineral coatings are generally <5 μm thick. Although the available reactive surface area of Fe^0 has been reduced through time near the upgradient PRB edge where the greatest amount of Cr accumulation occurs, some of the secondary mineral precipitates identified (mackinawite, carbonate green rust, magnetite) also support Cr redox transformation and uptake, thus potentially compensating for losses in iron metal reactivity due to surface precipitation.

Semiquantitative energy-dispersive X-ray analysis indicates a strong correlation between Fe and Cr. Where detected by X-ray analysis, however, Cr is associated with iron sulfide

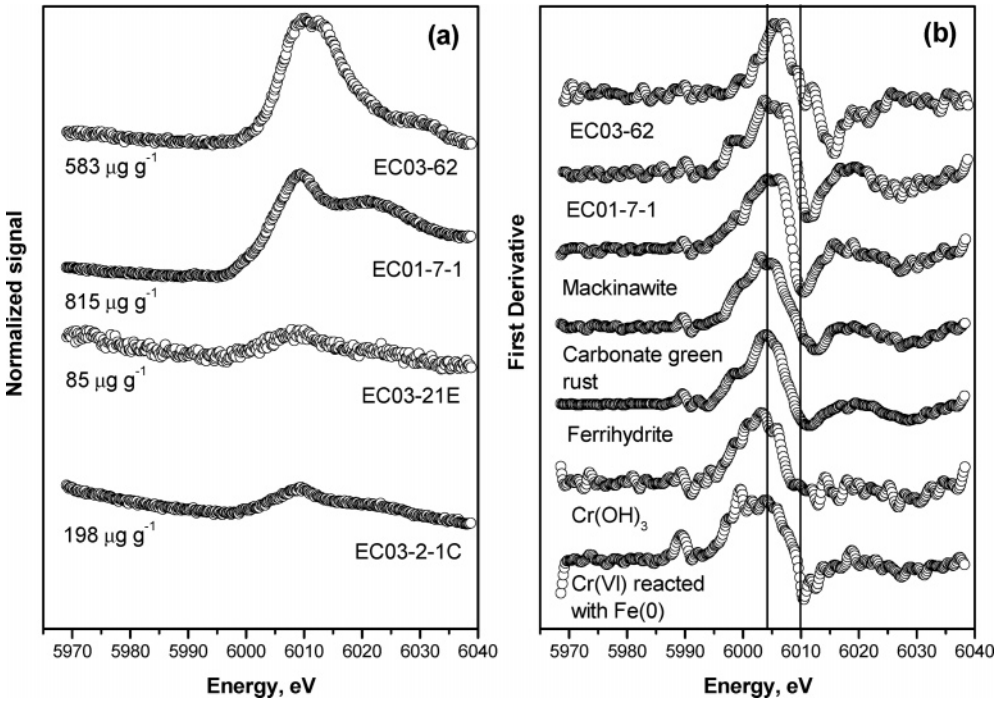

FIGURE 5. (a) Chromium K-edge XANES spectra of samples collected from the Elizabeth City site with Cr concentrations and (b) first derivative spectra for selected reference compounds and field samples.

TABLE 1. Selected Characteristics of Four Samples Collected from the Zerovalent Iron PRB Located near Elizabeth City, NC

sample	Cr[a] (μg g^{-1})	Cr K edge[b] (eV)	inorganic carbon[c] (μg g^{-1})	total sulfur[c] (μg g^{-1})	Fe[a] (wt %)	location
EC03-62	583	6005	546	861	10.3	aquifer 40 cm upgradient of PRB
EC01-7-1	815	6004	1545	1610	12.8	within PRB, fine-grained materials
EC03-21E	85	6005	2423	811	3.7	aquifer 10 cm upgradient of PRB
EC03-2-1 C	198	6004	1027	306	30.9	within PRB, fine-grained materials

[a] Measured by ICP-OES after microwave-assisted digestion in nitric acid. [b] Chromium K-edge XANES spectra shown in Figure 5a. [c] Measured by coulometric methods.

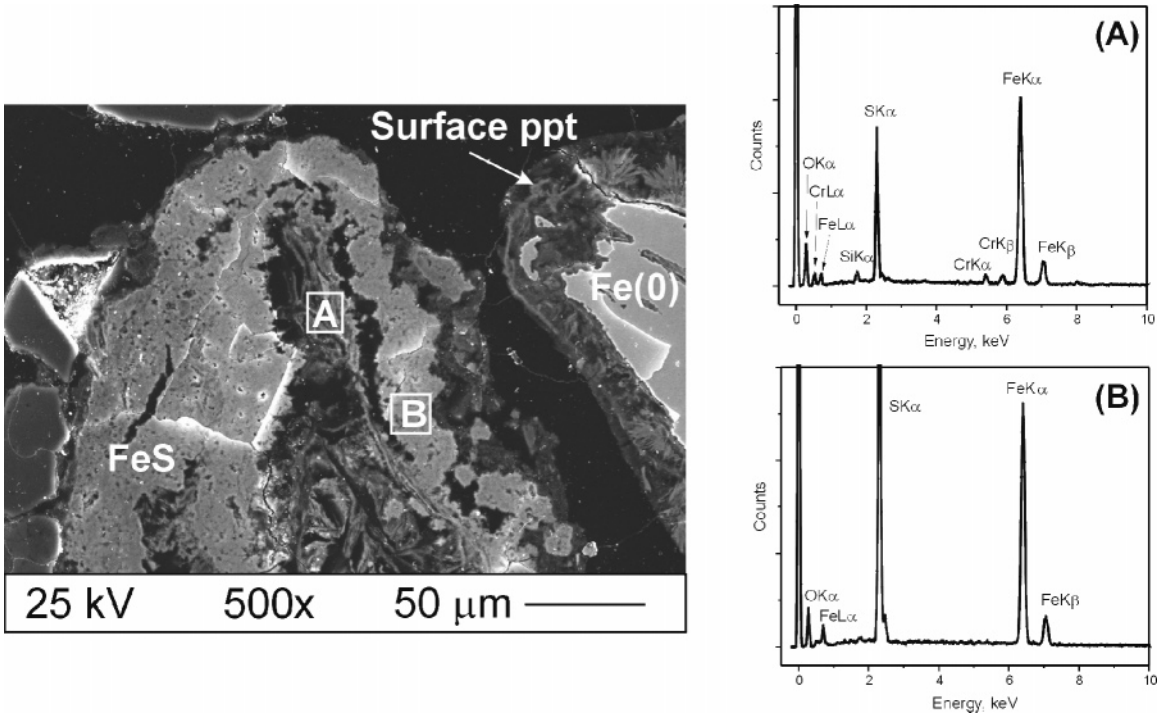

FIGURE 6. SEM photomicrograph of FeS grain and Fe(0) grain with surface precipitates. EDX spectra shown for region A and B. In region A, semiquantitative results indicate a Cr concentration of 1.9 wt %.

grains, a finding in parallel with the results obtained using the first-derivative XANES analysis (Figure 6). The observed correlation between Cr and FeS suggests that chromium uptake processes involving surfaces other than ZVI may be important in field-scale PRB installations. Cr removal in the ZVI PRB at Elizabeth City is in part governed by the geochemical environment established by corroding iron granules (i.e., moderately alkaline and reducing conditions) and not solely by interactions with the emplaced reactive medium. For example, EDX results generally show nondetectable Cr concentrations (<0.25 wt %) in the surface precipitates that coat iron granules. Experimental studies have shown that mackinawite has a large capacity for reducing Cr(VI) to insoluble Cr(III) compounds (*44*, *46*), and data presented in Figures 5b and 6 provide evidence for the environmental relevance of this process. The proposed mechanism for chromate removal by mackinawite is a surface precipitation process resulting in the composition $[Cr_{0.75}Fe_{0.25}](OH)_3$ (ref *44*). It is likely that Cr is also associated with other neoformed iron-bearing mineral phases in addition to mackinawite; however, so far our studies have not revealed other clear relationships. Microscopy-based X-ray absorption spectroscopic studies are planned to provide more details of Cr associations in the solid phase.

Solubility Evaluation. Insight into the processes controlling Cr removal can also be evaluated by comparing aqueous concentrations with the predicted pH solubility of Cr-bearing compounds. The XANES data presented in Figure 5a demonstrate that Cr is present in the solid phase in the trivalent form. In Figure 7, pH-dependent solubilities of Cr(III) phases Cr_2O_3 and $Cr(OH)_3$ are compared to groundwater Cr concentrations, corrected to activities using the Davies equation (*47*). Note that Cr hydroxide is metastable compared to Cr trioxide. Nevertheless, field data cluster around and just below the predicted solubility of $Cr(OH)_3$ and are vastly oversaturated with respect to Cr_2O_3. Also shown are two different groups of data, separated in pH, and representative of the PRB environment and the aquifer immediately upgradient and downgradient of the PRB, respectively (Figure 7). In both environments, XANES analysis indicates the predominance of Cr(III) in the solid phase and aqueous concentrations are undersaturated with respect to Cr hydroxide, generally within a factor of 50× the predicted solubility of pure $Cr(OH)_3$. The observed concentration trends might be consistent with the presence of a mixed Fe−Cr phase (*48*), e.g., such as the surface precipitates on mackinawite described by Patterson et al. (ref *44*). However, available experimental data on the solubility of mixed Cr−Fe solids are limited to pH conditions below 5 (*48*).

Implications: Stability and Capacity. Data in Figure 7 suggest that the solubility of $Cr(OH)_3$ is a conservative estimate of Cr concentrations that can be achieved in ZVI PRBs. Following from this observation is the conclusion that Cr is expected to be stable in the solid phase (aqueous concentrations less than 10^{-6} M) as long as pH conditions stay within a range from about 5 to 11 and redox conditions

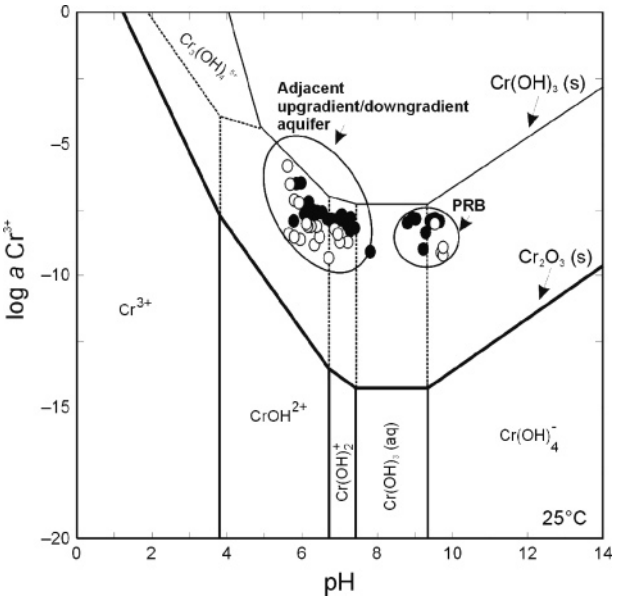

FIGURE 7. Activity of Cr as a function of pH determined in groundwater from Elizabeth City (open circles, 2003; closed circles, 2004) compared to the predicted solubility of $Cr(OH)_3$ and Cr_2O_3 (thermodynamic data in Supporting Information, Table S2). Groundwater samples containing Cr(VI) are not plotted.

remain moderately reducing to prevent oxidation of Cr(III) to Cr(VI). Results of this study indicate that the capacity of zerovalent iron systems to remediate Cr in groundwater is greater than what might be achieved based on considering the iron metal contribution to Cr removal alone. This enhanced capacity comes about from the formation of specific iron corrosion products precipitated via abiotic (e.g., green rust) or microbially mediated reactions (e.g., mackinawite) that augment and perhaps control Cr removal. Another potential source of reductive capacity and expanded treatment coverage in the subsurface stems from the buildup of Fe(II) in solution from ZVI corrosion and dissolution of neoformed Fe(II)-bearing mineral phases (*49*−*51*). The importance of coupled biotic−abiotic reduction pathways of Cr(VI) in subsurface environments involving Fe(II) solids and aqueous species has been previously discussed (*52*, *53*). However, consideration of the enhanced effect of secondary mineralization on contaminant removal should be incorporated into system designs for groundwater restoration and models that attempt to predict the longevity of ZVI systems used for groundwater cleanup. The relative contribution of these processes in remedial applications will depend on, for example, the rate of secondary mineral accumulation, the specific capacity of secondary minerals for Cr removal, and the transport of Cr to sites of uptake. These factors can all be assessed in subsurface monitoring programs.

Acknowledgments

The U.S. Environmental Protection Agency through its Office of Research and Development funded the research described here. It has not been subjected to Agency review and therefore does not necessarily reflect the views of the Agency, and no official endorsement should be inferred. Mention of trade names or commercial products does not constitute endorsement or recommendation for use. We gratefully acknowledge the analytical support provided by Ning Xu and Sandra Saye of Shaw Environmental (Contract No. 68-C-03-097) and F. Beck and P. Clark for field assistance. Use of the Advanced Photon Source is supported by the U.S. Department of Energy, Office of Science, Office of Basic Energy Sciences, under Contract No. W-31-109-Eng-38. PNC-CAT facilities at the Advanced Photon Source, and research at these facilities, are supported by the US DOE Office of Science Grant No. DEFG03-97ER45628, the University of Washington, a major facilities access grant from NSERC, Simon Fraser University, and the Advanced Photon Source.

Supporting Information Available

Additional information on the preparation of reference materials used in the XANES analysis (Table S1 and Figure S1), site characterization data (Figure S2), and thermodynamic data used for modeling chromium speciation and calculating saturation indices (Table S2). This material is available free of charge via the Internet at http://pubs.acs.org.

Literature Cited

(1) U.S. Environmental Protection Agency. *Economic Analysis of the Implementation of Permeable Reactive Barriers for Remediation of Contaminated Groundwater*, EPA/600/R-02/034; U.S. EPA: Washington, DC, 2002.
(2) Gavaskar, A. R.; Gupta, N.; Sass, B. M.; Jansoy, R. J.; O'Sullivan, D. *Permeable Reactive Barriers for Groundwater Remediation: Design, Construction, and Monitoring*; Battelle Press: Ohio, 1998.
(3) Blowes, D. W.; Ptacek, C. J.; Benner, S. G.; McRae, C.; Bennett, T. A.; Puls, R. W. Treatment of inorganic contaminants using permeable reactive barriers. *J. Contam. Hydrol.* **2000**, *45*, 123−137.
(4) U. S. Environmental Protection Agency. *An In Situ Permeable Reactive Barrier for the Treatment of Hexavalent Chromium and Trichloroethylene in Groundwater*, EPA/600/R-99/095a; U.S. EPA: Washington, DC, 1999.
(5) Puls, R. W.; Blowes, D. W.; Gillham, R. W. Long-term performance monitoring for a permeable reactive barrier at the U. S. Coast Guard Support Center, Elizabeth City, North Carolina. *J. Hazard. Mater.* **1999**, *68*, 109−124.
(6) Kjeldsen, P.; Locht, T. Removal of chromate in a permeable reactive barrier using zerovalent iron. In *Groundwater Quality; Natural and Enhanced Restoration of Groundwater Pollution*; Thornton, S. F., Oswald, S. E., Eds.; IAHS-AISH Publication, 2002; Vol. 275, pp 409−414.
(7) Morrison, S. J.; Metzler, D. R.; Carpenter, C. E. Uranium precipitation in a permeable reactive barrier by progressive irreversible dissolution of zerovalent iron. *Environ. Sci. Technol.* **2001**, *35*, 385−390.
(8) Gu, B.; Watson, D. B.; Phillips, D. H.; Liang, L. In *Handbook of Groundwater Remediation Using Permeable Reactive Barriers;* Naftz, D., Morrison, S., Fuller, C., Davis, J., Eds.; Academic Press: Amsterdam, 2002; pp 305−342.
(9) Gould, J. P. The kinetics of hexavalent chromium reduction by metallic iron. *Water Res.* **1982**, *16*, 861−877.
(10) Cantrell, K. J.; Kaplan, D. I.; Wietsma, T. W. Zerovalent iron for the in situ remediation of selected metals in groundwater. *J. Hazard. Mater.* **1995**, *42*, 201−212.
(11) Powell, R. M.; Puls, R. W.; Hightower, S. K.; Sabatini, D. A. Coupled iron corrosion and chromate reduction: Mechanisms for subsurface remediation. *Environ. Sci. Technol.* **1995**, *29*, 1913−1922.
(12) Blowes, D. W.; Ptacek, C. J.; Jambor, J. L. In situ remediation of Cr(VI)-contaminated groundwater using permeable reactive walls: laboratory studies. *Environ. Sci. Technol.* **1997**, *31*, 3348−3357.
(13) Pratt, A. R.; Blowes, D. W.; Ptacek, C. J. Products of chromate reduction on proposed subsurface remediation material. *Environ. Sci. Technol.* **1997**, *31*, 2492−2498.
(14) Melitas, N.; Chuffe-Moscoso, O.; Farrell, J. Kinetics of soluble chromium removal from contaminated water by zerovalent iron media: corrosion inhibition and passive oxide effects. *Environ. Sci. Technol.* **2001**, *35*, 3948−3953.
(15) Alowitz, M. J.; Scherer, M. M. Kinetics of nitrate, nitrite, and Cr(VI) reduction by iron metal. *Environ. Sci. Technol.* **2002**, *36*, 299−306.
(16) Gandhi, S.; Oh, B.-T.; Schnoor, J. L.; Alvarez, P. J. J. Degradation of TCE, Cr(VI), sulfate, and nitrate mixtures by granular iron in flow-through columns under different microbial conditions. *Water Res.* **2002**, *36*, 1973−1982.
(17) Singh, I. B.; Singh, D. R. Effects of pH in Cr−Fe interaction during Cr(VI) removal by metallic iron. *Environ. Technol.* **2003**, *24*, 1041−1047.
(18) Fiedor, J. N.; Bostick, W. D.; Jarabek, R. J.; Farrell, J. Understanding the mechanism of uranium removal from groundwater

by zerovalent iron using X-ray photoelectron spectroscopy. *Environ. Sci. Technol.* **1998**, *32*, 1466−1473.
(19) Gu, B.; Liang, L.; Dickey, M. J.; Yin, X.; Dai, S. Reductive precipitation of U(IV) by zerovalent iron. *Environ. Sci. Technol.* **1998**, *32*, 3366−3373.
(20) Lackovic, J. A.; Nikolaidis, N. P.; Dobbs, G. M. Inorganic arsenic removal by zerovalent iron. *Environ. Eng. Sci.* **2000**, *17*, 29−39.
(21) Farrell, J.; Wang, J.; O'Day, P.; Conklin, M. Electrochemical and spectroscopic study of arsenate removal from water using zerovalent iron media. *Environ. Sci. Technol.* **2001**, *35*, 2026−2032.
(22) Manning, B. A.; Hunt, M. L.; Amrhein, C.; Yarmoff, J. A. Arsenic-(III) and arsenic(V) reactions with zerovalent iron corrosion products. *Environ. Sci. Technol.* **2002**, *36*, 5455−5461.
(23) Su, C.; Puls, R. W. Arsenate and arsenite removal by zerovalent iron: kinetics, redox transformation, and implications for in situ groundwater remediation. *Environ. Sci. Technol.* **2001**, *35*, 1487−1492.
(24) Lien, H.-L.; Wilkin, R. T. High-level arsenite removal from groundwater by zerovalent iron. *Chemosphere* **2005**, *59*, 377−386.
(25) Shokes, T. E.; Möller, G. Removal of dissolved heavy metals from acid rock drainage using iron metal. *Environ. Sci. Technol.* **1999**, *33*, 282−287.
(26) Wilkin, R. T.; McNeil, M. S. Laboratory evaluation of zerovalent iron to treat water impacted by acid mine drainage. *Chemosphere* **2003**, *53*, 715−725.
(27) Herbert, R. B. Zinc immobilization by zerovalent Fe: surface chemistry and mineralogy of reaction products. *Mineral. Magn.* **2003**, *67*, 1285−1298.
(28) Gu, B.; Phelps, T. J.; Liang, L.; Dickey, M. J.; Roh, Y.; Kinsall, B. L.; Palumbo, A. V.; Jacobs, G. K. Biogeochemical dynamics in zerovalent iron columns: implications for permeable reactive barriers. *Environ. Sci. Technol.* **1999**, *33*, 2170−2177.
(29) Roh, Y.; Lee, S. Y.; Elless, M. P. Characterization of corrosion products in the permeable reactive barriers. *Environ. Geol.* **2000**, *40*, 184−194.
(30) Furukawa, Y.; Wook, J.; Watkins, J.; Wilkin, R. T. Formation of ferrihydrite and associated iron corrosion products in permeable reactive barriers of zerovalent iron. *Environ. Sci. Technol.* **2002**, *36*, 5469−5475.
(31) Wilkin, R. T.; Puls, R. W.; Sewell, G. W. Long-term performance of permeable reactive barriers using zerovalent iron: geochemical and microbiological effects. *Ground Water* **2003**, *41*, 493−503.
(32) Phillips, D. H.; Watson, D. B.; Roh, Y.; Gu, B. Mineralogical characteristics and transformations during long-term operation of a zerovalent iron reactive barrier. *J. Environ. Qual.* **2003**, *32*, 2033−2045.
(33) Kamolpornwijit, W.; Liang, L.; Moline, G. R.; Hart, T.; West, O. R. Identification and quantification of mineral precipitation in Fe^0 filings from a column study. *Environ. Sci. Technol.* **2004**, *38*, 5757−5765.
(34) Mayer, K. U.; Blowes, D. W.; Frind, E. O. Reactive transport modeling of an in situ reactive barrier for the treatment of hexavalent chromium and trichloroethylene in groundwater. *Water Resour. Res.* **2001**, *37*, 3091−3103.
(35) U. S. Environmental Protection Agency. *Capstone Report on the Application, Monitoring, and Performance of Permeable Reactive Barriers for Groundwater Remediation, Volume 1: Performance Evaluations at Two Sites*, EPA/600/R-03/045a; U.S. EPA: Washington, DC, 2003.
(36) Beck, F. P.; Puls, R. W.; Clark, P. J. Direct push methods for locating and collecting cores of aquifer sediment and zerovalent iron from a permeable reactive barrier. *Groundwater Monit. Rem.* **2002**, *22*, 165−168.
(37) U. S. Environmental Protection Agency. *Capstone Report on the Application, Monitoring, and Performance of Permeable Reactive Barriers for Groundwater Remediation, Volume 2: Soil and Groundwater Sampling*, EPA/600/R-03/045b; U.S. EPA: Washington, DC, 2003.
(38) Scherer, M. M.; Richter, S.; Valentine, R. L.; Alvarez, P. Chemistry and microbiology of permeable reactive barriers for in situ groundwater cleanup. *Crit. Rev. Environ. Sci. Technol.* **2000**, *30*, 363−411.
(39) Scherer, M. M.; Balko, B. A.; Tratnyek, P. G. The role of oxides in reduction reactions at the metal-water interface. In *Kinetics and Mechanisms of Reactions at the Mineral-Water Interface*; Sparks, D. L., Grundl, T., Eds.; American Chemical Society, Washington, DC, 1998; Chapter 15.
(40) Liang, L.; Puls, R. W.; Korte, N.; Reeter, C.; Gu, B. Geochemical and microbiological reactions affecting the long-term performance of in situ barriers. *Adv. Environ. Res.* **2000**, *4*, 273−286.
(41) Bond, D. L.; Fendorf, S. Kinetics and structural constraints of chromate reduction by green rusts. *Environ. Sci. Technol.* **2003**, *37*, 2750−2757.
(42) Legrand, L.; Figuigui, A.; Mercier, F.; Chausse, A. Reduction of aqueous chromate by Fe(II)/Fe(III) carbonate green rust: kinetic and mechanistic studies. *Environ. Sci. Technol.* **2004**, *38*, 4587−4595.
(43) Loyaux-Lawniczack, S.; Refait, Ph.; Ehrhardt, J.-J.; Lecomte, P.; Genin, J. M. Trapping of Cr by formation of ferrihydrite during the reduction of chromate ions by Fe(II)−Fe(III) hydroxysalt green rusts. *Environ. Sci. Technol.* **2000**, *34*, 438−443.
(44) Patterson, R. R.; Fendorf, S.; Fendorf, M. Reduction of hexavalent chromium by amorphous iron sulfide. *Environ. Sci. Technol.* **1997**, *31*, 2039−2044.
(45) Doyle, C. S.; Kendelewicz, T.; Bostick, B. C.; Brown, G. E. Soft X-ray spectroscopic studies of the reaction of fractured pyrite surfaces with Cr(VI)-containing aqueous solutions. *Geochim. Cosmochim. Acta* **2004**, *68*, 4287−4299.
(46) Mullet, M.; Boursiquot, S.; Ehrhardt, J.-J. Removal of hexavalent chromium from solutions by mackinawite, tetragonal FeS. *Colloids Surf., A* **2004**, *244*, 77−85.
(47) Stumm, W.; Morgan, J. J. *Aquatic Chemistry*, 2nd ed.; John Wiley and Sons: New York, 1981.
(48) Sass, B. M.; Rai, D. Solubility of amorphous chromium(III)-iron(III) hydroxide solutions. *Inorg. Chem.* **1987**, *26*, 2228−2232.
(49) Sedlak, D. L.; Chan, P. G. The reduction of Cr(VI) by Fe(II) in natural waters. *Geochim. Cosmochim. Acta* **1997**, *61*, 2185−2192.
(50) Pettine, M.; Dottone, L.; Campanella, L.; Millero, F. J.; Passino, R. The reduction of chromium(VI) by iron(II) in aqueous solutions. *Geochim. Cosmochim. Acta* **1998**, *62*, 1509−1519.
(51) Fendorf, S. E.; Li, G. Kinetics of chromate reduction reduction by ferrous iron. *Environ. Sci. Technol.* **1996**, *30*, 1614−1617.
(52) Hwang, I.; Batchelor, B.; Schlautman, M. A.; Wang, R. Effects of ferrous iron and molecular oxygen on chromium(VI) redox kinetics in the presence of aquifer solids. *J. Hazard. Mater.* **2002**, *B92*, 143−159.
(53) Hansel, C. M.; Weilinga, B. W.; Fendorf, S. Structural and compositional evolution of Cr/Fe solids after indirect chromate reduction by dissimilatory iron-reducing bacteria. *Geochim. Cosmochim. Acta* **2003**, *67*, 401−412.

Received for review January 24, 2005. Revised manuscript received April 4, 2005. Accepted April 5, 2005.

ES050157X